*Manuscript
Click here to download Manuscript: C_Demeure_2011_47513.doc

Early systemic bacterial dissemination and a rapid innate immune response characterize genetic resistance to plague of SEG mice

Christian E. Demeure[1], Charlène Blanchet[2], Catherine Fitting[3], Corinne Fayolle[1], Huot Khun[4], Marek Szatanik[2], Geneviève Milon[5], Jean-Jacques Panthier[2], Jean Jaubert[2], Xavier Montagutelli[2], Michel Huerre[4], Jean-Marc Cavaillon[3], and Elisabeth Carniel[1]

[1]*Yersinia* Research Unit

[2]Mouse Functional Genetics Unit

[3]Unité Cytokines et Inflammation

[4]Unité de recherche et d'expertise Histotechnologie et Pathologie

[5]Unité Immunophysiologie et Parasitisme Intracellulaire,

Institut Pasteur, 75724 Paris, France.

Abstract : 199 words

Text: 3473 words

Running Title: Innate immunity in plague resistant mice

Footnotes

Potential conflict of interest: none.

Financial support: This study was supported by a BIOTOX grant from the French Ministry of Health and a grant from Aventis Pharma (Sanofi-Aventis group) and Bayer Pharma as part of a multi-organism call for proposal. CB is a recipient of a DGA (*Délégation Générale pour l'Armement*) fellowship. The Mouse functional Genetics Unit was supported by Merck Serono.

Preliminary results of this work were presented by E. Carniel at the "9th International Symposium on Yersinia" (Oct. 10-14th, 2006) in Lexington, Kentucky.

New affiliations:

M. Szatanik: "Unité Postulante Infections Bactériennes Invasives", Institut Pasteur, 75724 Paris, France.

C. Blanchet: "Unité Cytokines et Inflammation", Institut Pasteur, 75724 Paris, France.

Corinne Fayolle: "Service de l'Enseignement", Institut Pasteur, 75724 Paris, France.

Reprints or correspondence: C.E. Demeure, *Yersinia* Research Unit, Institut Pasteur, 28 rue du Dr Roux, Paris 75724, France. E-mail: cdemeure@pasteur.fr, Tel: 33-1-45688448, Fax: 33-1-45688954

Abstract

***Background*:** While laboratory mice are usually highly susceptible to *Yersinia pestis*, we recently identified a mouse strain (SEG) that exhibited an exceptional capacity to resist bubonic plague and used it to identify immune mechanisms associated with resistance.

***Methods*:** The kinetics of infection, circulating blood cells, granulopoiesis, lesions and cellular populations in the spleen, and cytokine production in various tissues were compared in SEG and susceptible C57BL/6J mice after subcutaneous infection with the virulent *Y. pestis* CO92.

Results: Strikingly, bacterial invasion occurred early (day 2) but was transient in SEG/Pas, while in C57BL/6J it was delayed but continuous until death. The bacterial load in all organs significantly correlated with the production of five cytokines (G-CSF, KC, MCP-1, IL-1α and IL-6) involved in monocyte and neutrophil recruitment. Indeed, higher proportions of these two cell types in blood and massive recruitment of F4/80+CD11b- macrophages in spleen were observed in SEG/Pas at early time point (day 2). Later times post-infection (day 4) were characterized in C57BL/6J by destructive lesions of the spleen and impaired granulopoiesis.

***Conclusion*:** A fast and efficient *Y. pestis* dissemination in SEG may be critical for the triggering of an early and effective innate immune response necessary for surviving plague.

Keywords: *Yersinia pestis*, plague, *Mus spretus*, *Mus musculus*, dissemination, F4/80+ macrophages, Polymorphonuclear neutrophils.

INTRODUCTION

Plague has caused three pandemics that killed 200 millions of human beings [1, 2]. Despite considerable progresses in its prevention and cure, the disease persists today on three continents (Africa, Asia and America) [3] and has resurged in areas considered plague-free for several decades, leading to its categorization as a re-emerging disease [4]. This threat has been further exacerbated by the isolation of *Yersinia pestis* strains naturally resistant to antibiotics [5, 6], and by their potential use for bioterrorism.

Bubonic plague, the most common clinical presentation, results from the bite of infected fleas. After intradermal penetration, *Y. pestis* disseminates via lymphatic vessels to draining lymph nodes and then spread to various tissues (spleen, liver) before causing a fatal septicemia [7, 8]. Without prompt diagnosis and antibiotherapy, bubonic plague is rapidly lethal in 50-70% of cases [1]. Strikingly, little is known about the characteristics of the systemic and local host responses specifically targeted by *Y. pestis* during the infectious process.

During Middle Ages, some individuals were able to survive bubonic plague, suggesting a genetic determinism of resistance. Non-human mammalian species display variable levels of susceptibility to plague [1]. The host mechanisms responsible for these different responses are unknown but are most likely genetically determined. Even rodents, the major plague reservoir, display a wide susceptibility spectrum. The observation that the progeny of various rodent species trapped in plague foci is significantly more resistant to plague than their counterparts from non-plague foci [9-12], suggests the selection of protective allelic combinations under *Y. pestis* pressure.

Laboratory mice (*Mus musculus*), a widely used experimental model to study *Y. pestis* pathophysiology, are usually highly susceptible to plague (*Y. pestis* 50% lethal dose (LD_{50}) of ≈10 cfu upon subcutaneous (sc) infection) [13]. However, mice resisting an intravenous (iv) inoculation of high doses of *Y. pestis* KIM5 were recently reported [14, 15]. Genetic studies subsequently

showed that their resistance was at least in part associated with ≥30 cM of 129-derived genomic DNA near the *Il10* locus [16], or with the Major Histocompatibility Complex region on chromosome 17 [15]. Some resistant strains (129 substrain) displayed an acute inflammatory cellular response [17], and others (BALB/cJ) a lower production of IL-6 [15]. Although these studies brought valuable new information about genetic determinants and physiological mechanisms of resistance to plague, their drawback is that they used an attenuated *Y. pestis* KIM5 strain (deleted of the High-Pathogenicity Island) that had to be injected by a non-physiological route (iv). Actually, the 129 mice were as susceptible as other laboratory mice when a fully virulent *Y. pestis* was injected sc [17].

We recently showed that the SEG/Pas (SEG) mouse strain exhibits high resistance to a sc infection with a fully virulent *Y. pestis* [18]. This mouse strain (*Mus spretus*) is derived from wild progenitors and has been established as an inbred strain [19]. While 100 cfu killed 94% of the C57BL/6J animals (B6), only 10% of SEG mice succumbed. Furthermore, the LD_{50} of *Y. pestis* for B6 was 3.2 cfu, whereas that for SEG was $>10^7$ cfu [18]. The availability of this mouse strain provided a unique opportunity to identify pathophysiological mechanisms of resistance to plague, by comparing the infectious process and the host response in susceptible (B6) and resistant (SEG) animals.

MATERIALS AND METHODS

Bacterial growth conditions.

Y. pestis CO92 was grown in Luria-Bertani (LB) broth or on LB agar supplemented with 0.2% hemin for 48h at 28°C, in a BSL3 laboratory. Kinetics of bacterial growth in mouse serum were determined by inoculating 10^3 cfu/ml of CO92 grown at 37°C in undecomplemented pooled sera

from 7 mice. The sera were incubated at 37°C for 48h and aliquots were taken at various intervals, diluted and plated on LB-H.

Mouse experiments

Infection with *Y. pestis* was performed in a BSL3 animal facility, according to the Institut Pasteur guidelines. Groups of 8-12 weeks old female C57BL/6J (Charles River) or SEG/Pas (Institut Pasteur) received a sc injection of 100 cfu in the abdominal skin. Mortality was followed for 14 days. To study bacterial spread and host responses, groups of five mice were sacrificed on D1-4 post-infection (pi), and their blood, spleen, liver (one lobe), lungs, inguinal lymph nodes and femurs were collected. One half of the spleen and liver was fixed for immunohistological analyses, while the other half, the lungs and inguinal lymph nodes were homogenized using glass beads (VWR) to evaluate bacterial load. The remaining of supernatants of grinded organs and serum were sterile-filtered and frozen for cytokine measurement. Blood formula was determined using a Vet'ABC counter (SCIL).

Immunohistological analyses

Organs fixed with 4% paraformaldehyde were dehydrated and embedded in paraffin. Five micrometer sections were stained with hematoxylin and eosin. PMNs were quantified microscopically using a score ranging from 0 (normal) to 5 (large areas filled with infiltrating PMNs) and hemorrhages were scored from 0 (normal) to 3 (extended hemorrhages) on at least three complete sections per sample. For immunohistological labeling of bacteria, sections were incubated with a *Y. pestis* F1-specific rabbit antiserum (Institut Pasteur) followed by Rabbit specific Histofine® MAX-PO (Nichirei). Peroxidase was detected using the AEC substrate (Sigma) with hematoxylin counterstaining.

Cytokine/chemokine assays

Measurement of IL-1α, IL-1β, IL-10, TNFα, INFγ, IL-6, IL-12p70, G-CSF, KC, and MCP-1 was performed with the BioPlex cytokine bead array (Bio-Rad), using a Luminex platform.

Flow cytometry analyses

Minced bone marrow and spleen tissues were passed trough a 70 µm mesh (BD biosciences), and red cells were lyzed using Gey's method [20]. Polymorphonuclear neutrophils (PMN: CD11b+Ly6G^{hi}SSC^{hi}), T cells (TCR+), bone marrow monocytes (CD11b+Ly6G-SSC^{int}), spleen red pulp macrophages (F4/80+CD11b-Ly6G-) and other macrophages (CD11b+F4/80-Ly6G-) were quantified using specific fluorescent antibodies: anti-CD11b-Pacific Blue (eBiosciences), anti-TCRbeta-Alexa488, anti-F4/80-Allophycocyanin (Invitrogen), and anti-Ly6G-PE mAb clone 1A8 (BD Biosciences). Cells were analyzed with a CyAn cytometer (Beckman-Coulter).

Statistical analyses

Statistical analyses included the Mann-Whitney-Wilcoxon test (quantitative parameters), Spearman test (cfu and cytokine contents), and Fisher exact test (mortality).

RESULTS

Mouse infections

To compare the progression of the infection and the host response in susceptible and resistant mice, 29 SEG and 30 B6 animals were infected sc with 100 cfu of *Y. pestis* CO92. A group of 9-10 animals was kept to follow mortality over 14 days (mortality group), and the 20 remaining mice (study group) were distributed in four cages to be analyzed on D1 to D4 pi. Ascribing *a priori* a day of sacrifice to each group prevented the bias of selecting in the latest days the animals that better resisted the infection in the early phase.

In the mortality group, B6 started to develop clinical symptoms of infection and to die on D3 pi, and 18/20 were dead on D14. In contrast, SEG developed clinical signs of disease such as prostration and ruffled fur earlier (D2), but started to recover on D4, and 17/19 animals survived and looked healthy on D14. The difference in survival was highly significant ($p<0.0001$). Body weight variations correlated with symptoms. Body weight loss in B6 mice began on D3 and reached 10% on D4, while body weight of SEG mice remained constant (Supplementary Figure 1A).

In the study group, one B6 mouse died on D4, and therefore only 9 animals were available for study at this time point.

Comparison of the infectious process in SEG and B6

Bacterial loads in SEG and B6 followed clearly distinct kinetics over the four days study period. A few circulating *Y. pestis* cells were detected in the blood of both mouse strains on D1, but they reached much higher numbers in the blood of SEG on D2 (Figure 1A). However, bacteremia subsequently decreased in SEG while it increased in B6, so that similar cfu numbers were found on D3 in the blood of the two mouse strains. On D4, SEG had cleared circulating bacteria while the bacterial load had continued to rise in B6.

Remarkably, a similar higher bacterial load was observed in all collected organs of SEG (although statistically significant in the lungs only) on D2 (Figure 1 B-E). The bacterial loads then stabilized and started to decline in most SEG organs. In contrast *Y. pestis* numbers rose continuously in B6 tissues, so that much higher bacterial loads were found in all B6 tissues analyzed (except lungs) on D4. The kinetics of infection was highly reproducible for the two groups of mice during two independent experiments.

Therefore, both susceptible and resistant mice were efficiently colonized by *Y. pestis*, but SEG displayed an earlier bacterial invasion that was transient.

Y. pestis growth in serum of SEG and B6

Since one of the most remarkable differences between resistant and susceptible animals was the capacity of SEG to clear circulating bacteria, we questioned whether a bactericidal component with a higher activity or in greater amount could be present at homeostasis or produced during infection in the serum of resistant mice. The growth curves of *Y. pestis* were similar in the undecomplemented sera of the two mouse strains, before and two days post-infection (Supplementary Figure 1B), indicating that SEG resistance is not attributable to the presence or release of a circulating antibacterial compound.

SEG and B6 blood cell populations during the infectious process

As bacterial clearance from the blood stream may also result from a cell-mediated process, the circulating cell populations during the course of infection were analyzed in SEG and B6. A significant increase in blood leukocyte numbers was observed between D0 and D1 in both mouse strains ($p<0.02$). However, leukocytosis persisted in SEG but not in B6, so that a marked difference in blood leukocytes was observed on D4 (Figure 2Aa). The same trend was noted for platelets (Figure 2Ab), while erythrocyte counts remained stable (Figure 2Ac), showing the specific increase of some blood cell populations in SEG. Within the leukocyte populations, lymphocytes, monocytes and polymorphonuclear cells (PMN) numbers rose in the two mouse strains on D1-2 pi (Figure 2Ad-f). PMNs and monocytes (but not lymphocytes) continued to increase over the study period, moderately in B6 and much more significantly in SEG.

Since the marked difference in circulating PMN and monocytes on D4 could result from a more efficient hematopoiesis in SEG, we examined the bone marrow cell populations in the two mouse strains. Before infection, the total cell content in the femurs was significantly higher in B6 ($31\pm0.4\times10^6$) than in SEG ($21\pm1.9\times10^6$), probably because of the larger body size of B6 (19.8±0.6 g) than SEG (16.6±1.6 g). The percentages of PMNs and monocytes in the bone marrow were

nonetheless similar in the two species, but became significantly higher in SEG on D4 (Figure 2B), suggesting a more efficient bone marrow hematopoiesis at a late stage of infection in resistant mice.

Tissue lesions in infected B6 and SEG

The liver of the two mouse strains exhibited similar histological lesions (mild inflammation with occasional weak hemorrhages and PMN infiltrates), which were moderate at all time points (data not shown). In contrast, tissue lesions characterized by a mild inflammatory infiltrate primarily composed of PMNs were observed in the spleen of B6 and SEG on D1-2, and subsequently became more pronounced in B6 (Figure 3A). Hemorrhages appearing on D2 and increasing over time were always more important in B6 spleens. At late time points (D4), B6 spleens exhibited necrotic lesions destroying the red pulp (Figure 3Ba) and containing free bacteria (Figure 3Bc). In contrast, microabscesses appearing as rare and well contained round foci of PMN infiltration without necrosis started to develop on D4 in SEG spleens (Figure 3Bb), and bacteria were mostly found within these microabscesses (Figure 3Bd). The infectious course in SEG thus differs from that of B6 by less destructive lesions of the spleen and the capacity to circumscribe bacterial foci.

Spleen cell populations in uninfected or infected B6 and SEG mice

To further investigate the differences in spleen responses, groups of 6-7 B6 and SEG mice were sacrificed before infection or on D2 pi, and their spleen cell populations were analyzed. The experiments were done twice and the results were pooled.

In non-infected animals, total spleen cells were in higher numbers in B6, as expected from their larger spleen size (31±18 mg in B6 versus 16±4 mg in SEG). Both mouse strains had similar proportions of F4/80± CD11b+ macrophages and undetectable PMN (CD11b+ Ly6G+) levels (Figure 3C, diamonds). The main difference was a higher percentage of T cells in B6 and of F4/80+ CD11b- macrophages in SEG.

After two days of infection, total splenocytes increased in the two mouse groups, indicating an early cell recruitment (Figure 3C, circles). The drop in T lymphocytes percentages in both mouse groups demonstrated that this cell enrichment was not due to an adaptive response. The proportion of CD11b+ macrophages was not significantly affected by the infection. In agreement with our histological observations, the moderate recruitment of PMNs (≈1.5% of spleen cells) observed in the two mouse strains could not account for the increased spleen cellularity on D2. The major change in both infected mouse strains was a significant increase in the F4/80+ CD11b- macrophage population, which was considerably higher in SEG. Actually, this cell type represented 40% of the splenocytes in infected SEG spleen versus ≈15% in B6. Immunohistolabeling of the F4/80 antigen in spleen sections indicated that all F4/80+ macrophages were located in the red pulp (data not shown).

Therefore, SEG have a higher basal level of F4/80+ red pulp macrophages and they show a remarkable expansion during infection.

Kinetics of cytokine release in the blood and organs of SEG and B6

The production of ten cytokines known to participate to the innate immune response was quantified in the plasma, lymph nodes and spleen of SEG and B6 during the course of infection. Five cytokines (IFNγ, TNFα, IL-1β, IL-10 and IL-12p70) exhibited similar levels of production in the two mouse strains during the infectious process, despite higher levels of four of them in B6 plasma prior to infection (Supplementary Figure S2).

The other five cytokines (G-CSF, KC, MCP-1, IL-1α and IL-6) displayed a clearly different kinetics of production in the two mouse strains (Figure 4). Most remarkably, their levels were correlated in the three biological samples tested. The pattern in SEG was characterized by a peak of production in the plasma and lymph nodes on D2, and in the spleen on D3. The levels of these cytokines were significantly lower in the organs of B6 at the same time points. At a later stage of infection (D4), the amounts of these five cytokines started to decline in SEG organs, while they

continued to rise or remained high (MCP-1) in B6, so that higher levels were detected in the plasma and lymph nodes of B6 on D4.

Therefore, *Y. pestis* infection in resistant mice was characterized by a faster but transient production of G-CSF, KC, MCP-1, IL-1α and IL-6, while susceptible mice displayed a delayed but continuously increasing cytokine response.

Correlation between cytokine release and bacterial load in SEG and B6

Interestingly, the kinetics of production of these five cytokines in SEG and B6 seemed to parallel the bacterial loads observed in the two mouse strains. Since cfu and cytokine data were available for each individual animal, the association between the bacterial burden in the plasma, spleen and lymph nodes (whatever the infection day) and the release of the ten cytokines studied was investigated.

The levels of the five cytokines that were not differentially produced between B6 and SEG (IFNγ, TNFα, IL-1β, IL-10 and IL-12p70) were most often not correlated with bacterial loads (Table 1). In contrast, a remarkable and significant correlation was observed between the levels of G-CSF, KC, MCP-1, IL-1α and IL-6 and the number of bacteria present in most mouse organs (Table 1). This correlation was true for both SEG and B6.

Our results thus indicate that, even if the kinetics of production of these five cytokines differed between susceptible and resistant mice, both mouse strains have the capacity to develop the same cytokine response when exposed to similar bacterial loads.

DISCUSSION

The wild-derived SEG mouse strain naturally exhibits an exceptional capacity to resist an otherwise lethal subcutaneous infection with *Y. pestis* [18]. We took advantage of this

unprecedented ability to survive bubonic plague to study pathophysiological mechanisms and host responses associated with the resistance phenotype. To do so, the course of infection and innate immune response were compared in resistant SEG and susceptible B6 mouse strains. The most remarkable and unexpected feature that emerged from this comparison was that *Y. pestis* colonized rapidly and more efficiently the organs of resistant mice. This was evidenced by clinical symptoms of infection that appeared on D2 in SEG, and were retarded (D4) in B6.

The higher bacterial load in SEG on D2 was accompanied by a higher in situ production of five cytokines (G-CSF, KC, MCP-1, IL-1α and IL-6). This rapid cytokine release is most likely the direct consequence of the bacterial burden since we found a highly significant correlation between the number of cfu and cytokine levels in each organ of each individual mouse tested. Of note, this correlation was not observed for the other five cytokines analyzed (IFNγ, TNFα, IL-1β, IL-10 and IL-12p70). A characteristic of the former group is that, in addition to being produced by bone marrow derived cells, they all are also released by somatic cells such as endothelial cells, fibroblasts and keratinocytes. This points at stromal cells rather than immune cells as a potential source for the early and coordinate production of G-CSF, KC, MCP-1, IL-1α and IL-6 upon stimulation by *Y. pestis*.

This early release may explain the higher numbers of circulating blood monocytes and PMN in SEG on D2. Indeed, MCP-1 is one of the key chemokines that regulate migration and infiltration of monocytes/macrophages at inflammatory sites [21, 22]. G-CSF and IL-6 induce granulocyte mobilization from the bone marrow and their activation, differentiation, and survival [23-25], and KC and IL-1α promote their chemotaxis [26, 27]. Since neutrophils and monocytes are key components of the host innate response to many bacterial pathogens [28-30], they most likely participate actively to *Y. pestis* clearance from the blood of SEG.

The early time points of infection in SEG were also characterized by a massive and specific expansion of F4/80+ CD11b- macrophages in the spleen, an organ important for capturing circulating bacteria. F4/80+ CD11b- macrophages reside in the liver (Kupffer cells) and the spleen,

in which they are restricted to the red pulp. Therefore, in contrast to CD11b+ macrophages, they are not in contact with lymphocytes and thus are not key players of the adaptive immunity. They are rather effectors of the innate response by phagocytosing blood bacteria penetrating into the highly vascularized red pulp of the spleen and by producing microbicidal metabolites [31]. F4/80+ CD11b- macrophages may thus be critical for the ability of SEG to respond rapidly and efficiently to a *Y. pestis* infection. An afflux of spleen macrophages was not observed in resistant 129 mice [17], indicating a distinct innate response in these mice. It is worth noting that the proportion of this subpopulation was already higher in SEG than B6 prior to infection, suggesting that SEG are already 'pre-programmed' to mount a more efficient F4/80+ CD11b- mediated cellular response.

D2 appears as a critical time point at which the host response is already committed to resistance or susceptibility. The differences observed later during infection (D3-4) may therefore simply reflect the consequences of an engagement of the host response towards bacterial clearance or multiplication. Indeed, later time points showed the containment and progressive decrease of the bacterial load in SEG (with a complete recovery of most animals), and a continuous increase of the bacterial burden in B6, followed by their death. The more abundant hematopoiesis and circulating blood cells observed in SEG on D4, as well as their capacity to trap spleen bacteria within a cellular reaction preventing massive destructive lesions, may thus reflect the results of the early triggering of an efficient innate immune response in resistant animals rather than being the cause of their recovery. Also arguing for the earliness of the response as being crucial for resistance is our observation that the two mouse strains had the capacity to elicit the same effective G-CSF, KC, MCP-1, IL-1α and IL-6 responses when exposed to comparable bacterial loads. This would be supported by the fact that, except for the IL-6R gene, no genetic determinant corresponding to these five cytokines is located on the three mouse chromosomal loci recently shown by us to be associated with SEG resistance to plague [18]. Thus, the major difference between B6 and SEG is not the quality of their cytokine responses, but the time at which they are triggered.

In conclusion, comparison of the *Y. pestis* infection course and innate immune response in susceptible and resistant mouse strains has shown that unexpectedly, the more efficient colonization of SEG by *Y. pestis* early during the infectious process may be critical for the triggering of an effective innate immune response.

Funding

This study was supported by a BIOTOX grant from the French Ministry of Health and a grant from Aventis Pharma (Sanofi-Aventis group) and Bayer Pharma as part of a multi-organism call for proposal. CB is a recipient of a DGA (*Délégation Générale pour l'Armement*) fellowship. The Mouse functional Genetics Unit is supported by Merck Serono.

Acknowledgements

The authors wish to thank Professor J.L. Guénet for his support to the project and A. Ferreira for help with flow cytometry.

Conflict of Interest

The authors have no conflicts of interest.

References

1. Perry RD, Fetherston JD. *Yersinia pestis*--etiologic agent of plague. Clin Microbiol Rev **1997**; 10:35-66.

2. Inglesby TV, Dennis DT, Henderson DA, et al. Plague as a biological weapon - Medical and public health management. J Am Med Assoc **2000**; 283:2281-90.

3. WHO. Human plague in 2002 and 2003. Wkly Epidemiol Rec **2004**; 79:301-8.

4. WHO. International meeting on preventing and controlling plague: the old calamity still has a future. Wkly Epidemiol Rec **2006**; 81:278-84.

5. Guiyoule A, Gerbaud G, Buchrieser C, et al. Transferable plasmid-mediated resistance to streptomycin in a clinical isolate of *Yersinia pestis*. Emerg Infect Dis **2001**; 7:43-8.

6. Galimand M, Guiyoule A, Gerbaud G, et al. Multidrug resistance in *Yersinia pestis* mediated by a transferable plasmid. N Engl J Med **1997**; 337:677-80.

7. Guinet F, Ave P, Jones L, Huerre M, Carniel E. Defective innate cell response and lymph node infiltration specify Yersinia pestis infection. PLoS One **2008**; 3:e1688.

8. Sebbane F, Gardner D, Long D, Gowen BB, Hinnebusch BJ. Kinetics of disease progression and host response in a rat model of bubonic plague. Am J Pathol **2005**; 166:1427-39.

9. Thomas RE, Barnes AM, Quan TJ, Beard ML, Carter LG, Hopla CE. Susceptibility to *Yersinia pestis* in the northern grasshopper mouse (Onychomys leucogaster). J Wildl Dis **1988**; 24:327-33.

10. Rahalison L, Ranjalahy M, Duplantier JM, et al. Susceptibility to plague of the rodents in Antananarivo Madagascar. The Genus Yersinia. Vol. 529. New York: Kluwer Academis/Plenum Publishers, **2003**. 439-442

11. Quan SF, Kartman L. Ecological studies of wild rodent plague in the San Francisco bay area of California. VIII. Susceptibilité of Wild Rodents to Experimental Plague Infection. Zoonoses Research **1962**; 1:121-44.

12. Hubbert WT, Goldenberg MI. Natural resistance to plague: genetic basis in the vole (Microtus californicus). Am J Trop Med Hyg **1970**; 19:1015-9.

13. Russel P, Eley SM, Hibbs SE, Manchee RJ, Stagg AJ, Titball RW. A comparison of Plague vaccine, USP and EV76 vaccine induced protection against *Yersinia pestis* in a murine model. Vaccine **1995**; 13:1551-6.

14. Philipovskiy AV, Cowan C, Wulff-Strobel CR, et al. Antibody against V antigen prevents Yop-dependent growth of *Yersinia pestis*. Infect Immun **2005**; 73:1532-42.

15. Turner JK, McAllister MM, Xu JL, Tapping RI. The resistance of BALB/cJ mice to *Yersinia pestis* maps to the major histocompatibility complex of chromosome 17. Infect Immun **2008**; 76:4092-9.

16. Turner JK, Xu JL, Tapping RI. Substrains of 129 Mice Are Resistant to *Yersinia pestis* KIM5: Implications for Interleukin-10-Deficient Mice. Infect Immun **2009**; 77:367-73.

17. Congleton YH, Wulff CR, Kerschen EJ, Straley SC. Mice naturally resistant to *Yersinia pestis* Delta pgm strains commonly used in pathogenicity studies. Infect Immun **2006**; 74:6501-4.

18. Blanchet C, Jaubert J, Carniel E, et al. Mus spretus SEG/Pas mice resist virulent Yersinia pestis, under multigenic control. Genes Immun **2011**; 12:23-30.

19. Guenet JL, Bonhomme F. Wild mice: an ever-increasing contribution to a popular mammalian model. Trends Genet **2003**; 19:24-31.

20. Mishell B, Shiigi S. Selected Methods in Cellular Immunology. San Francisco: W.H. Freeman and Co, **1980**.

21. Serbina NV, Pamer EG. Monocyte emigration from bone marrow during bacterial infection requires signals mediated by chemokine receptor CCR2. Nat Immunol **2006**; 7:311-7.

22. Deshmane SL, Kremlev S, Amini S, Sawaya BE. Monocyte chemoattractant protein-1 (MCP-1): an overview. J Interferon Cytokine Res **2009**; 29:313-26.

23. Semerad CL, Liu F, Gregory AD, Stumpf K, Link DC. G-CSF is an essential regulator of neutrophil trafficking from the bone marrow to the blood. Immunity **2002**; 17:413-23.

24. Walker F, Zhang HH, Matthews V, et al. IL6/sIL6R complex contributes to emergency granulopoietic responses in G-CSF- and GM-CSF-deficient mice. Blood **2008**; 111:3978-85.

25. Maianski NA, Mul FP, van Buul JD, Roos D, Kuijpers TW. Granulocyte colony-stimulating factor inhibits the mitochondria-dependent activation of caspase-3 in neutrophils. Blood **2002**; 99:672-9.

26. Ozaki Y, Ohashi T, Kume S. Potentiation of neutrophil function by recombinant DNA-produced interleukin 1a. J Leukoc Biol **1987**; 42:621-7.

27. Lira SA, Zalamea P, Heinrich JN, et al. Expression of the chemokine N51/KC in the thymus and epidermis of transgenic mice results in marked infiltration of a single class of inflammatory cells. J Exp Med **1994**; 180:2039-48.

28. Segal AW. How neutrophils kill microbes. Annu Rev Immunol **2005**; 23:197-223.

426 29. Serbina NV, Salazar-Mather TP, Biron CA, Kuziel WA, Pamer EG. TNF/iNOS-producing
427 dendritic cells mediate innate immune defense against bacterial infection. Immunity **2003**;
428 19:59-70.
429 30. Goodyear A, Jones A, Troyer R, Bielefeldt-Ohmann H, Dow S. Critical Protective Role for
430 MCP-1 in Pneumonic Burkholderia mallei Infection. J Immunol **2009**. 1445-54.
431 31. Adams DO, Hamilton TA. The cell biology of macrophage activation. Annu Rev Immunol
432 **1984**; 2:283-318.
433
434
435

436 **LEGEND TO FIGURES**

437

438 **Figure 1: Bacterial loads at different time points in the blood and organs of *Y. pestis*-infected**
439 **B6 and SEG.** Mice were infected sc with 100 cfu of CO92 and groups of 10 animals (combined
440 results of two independent experiments) were sacrificed on D1 to D4 pi. The bacterial loads in the
441 blood (cfu/ml), lymph nodes (cfu/2 lymph nodes), spleen, liver and lungs (cfu/g of tissue) were
442 determined for each animal and at each time point. Shown are means ± s.e.m. of 9-10 mice per
443 point. Statistical differences between the two mouse strains at each time point were evaluated using
444 the Mann-Whitney-Wilcoxon rank sum test and are indicated by stars. *: $p<0.05$; **: $p<0.01$.

445

446 **Figure 2: Blood (A) and bone marrow (B) cell numbers during the course of infection in SEG**
447 **and B6.** Shown are the means ± s.e.m. for 9-10 mice mice (blood) or 5 mice (bone marrow) at each
448 time point. Statistical differences between the two mouse strains at each time point were evaluated
449 using the Mann-Whitney-Wilcoxon rank sum test. *: $p<0.05$, **: $p<0.01$, ***: $p<0.001$.

450

451 **Figure 3: Tissue lesions and cell populations in the spleen of infected SEG and B6.**
452 (A) Number of animals with histological lesions (positive mice/total) in the spleen. Scores (means
453 ± s.e.m.) of hemorrhages (histological scale 0 to 3) and PMN infiltration (scale 0 to 5) and
454 summarize the observation of ≥60 microscopic fields (≥20 fields/section with a X20 objective on
455 ≥3 complete sections per sample). (B) Hematoxylin-Eosin (a, b) and anti-F1 immunohistochemical
456 staining (c, d) of spleen sections taken on D4 pi. B6 spleens had abundant foci of necrosis (small
457 arrows in a) containing numerous bacteria (red-brown color in c), while SEG spleens exhibited
458 some micro abscesses (large arrowhead in b) without necrosis and containing few bacteria (d). The
459 2-tailed non-parametric Mann-Whitney-Wilcoxon rank sum test was used to compare groups. *:
460 $p\leq0.05$, **: $p\leq0.01$. (C) Quantification of different spleen cell populations in B6 and SEG (12
461 animals each from two independent experiments, except for T cells where 7 animals were

analyzed). Splenocytes were counted microscopically and macrophages (MP), polymorphonuclear neutrophils (PMN) and T cells were quantified by flow cytometry. Individual results from uninfected (0, white diamonds) or infected (D2 pi, grey circles) animals are plotted. "+" on each side of the columns indicate mean values. The 2-tailed non-parametric Mann-Whitney-Wilcoxon rank sum test was used to compare groups. *: $p \leq 0.05$, **: $p \leq 0.01$, ***: $p \leq 0.001$.

Figure 4: Cytokine contents in the plasma, spleen and inguinal lymph nodes of B6 and SEG during the course of a *Y. pestis* infection. Shown are the values for five cytokines (G-CSF, KC, MCP-1, IL-1α and IL-6) in individual SEG (grey rectangles) and B6 (grey triangles) mice from D0 to D4 pi for 10 animals (9 for B6 on D4), and the median curves (plain lines for B6, and dotted lines for SEG). Groups were compared using the non-parametric Mann-Whitney-Wilcoxon rank sum test. *: $p \leq 0.05$; **: $p \leq 0.01$; ***: $p \leq 0.001$. Stars above the comparison bar indicate values significantly superior in SEG, while stars below the comparison bar indicate values significantly superior in B6.

Table 1. Correlation between bacterial load and cytokine content in tissues of infected mice

		SEG			B6		
		Plasma	Spleen	LN	Plasma	Spleen	LN
G-CSF	r:	0.50	0.67	0.45	0.69	0.68	0.57
	p:	0.0005	<0.0001	0.002	<0.0001	<0.0001	<0.0001
IL-1α	r:	0.41	0.57	0.39	0.57	0.55	0.50
	p:	0.005	<0.0001	0.009	<0.0001	0.0001	0.0005
IL-6	r:	0.52	0.54	nss	0.70	nss	0.54
	p:	0.0002	0.0001		<0.0001		0.0001
KC	r:	0.51	0.75	0.57	0.59	0.84	0.64
	p:	0.0003	<0.0001	<0.0001	<0.0001	<0.0001	<0.0001
MCP-1	r:	0.62	0.54	nss	0.71	0.42	0.45
	p:	<0.0001	0.0001		<0.0001	0.005	0.002
IL-1β	r:	nss	0.57	nss	nss	0.52	0.44
	p:		<0.0001			0.0003	0.003
IL-10	r:	nss	nss	nss	nss	nss	nss
	p:						
TNFα	r:	0.41	nss	nss	0.54	nss	nss
	p:	0.005			0.0002		
IFNγ	r:	nss	nss	nss	nss	nss	nss
	p:						
IL-12p70	r:	0.53	nss	nss	nss	nss	nss
	p:	0.0002					

NOTE: The non parametric Spearman rank test (r) was used to evaluate the correlation between cfu values and the level of each cytokine, regardless of the time pi. To account for multiple testing, a Bonferroni correction was applied so only correlation values with $p<0.01$ were retained, and in such cases both p and r values are given. Non statistically significant values were noted as nss. SEG samples: n=40, B6 samples: n=39. LN: lymph nodes.

Figure 1

Click here to download Figure: C_Demeure_2011_Fig.1_JID2.pdf

Figure 1

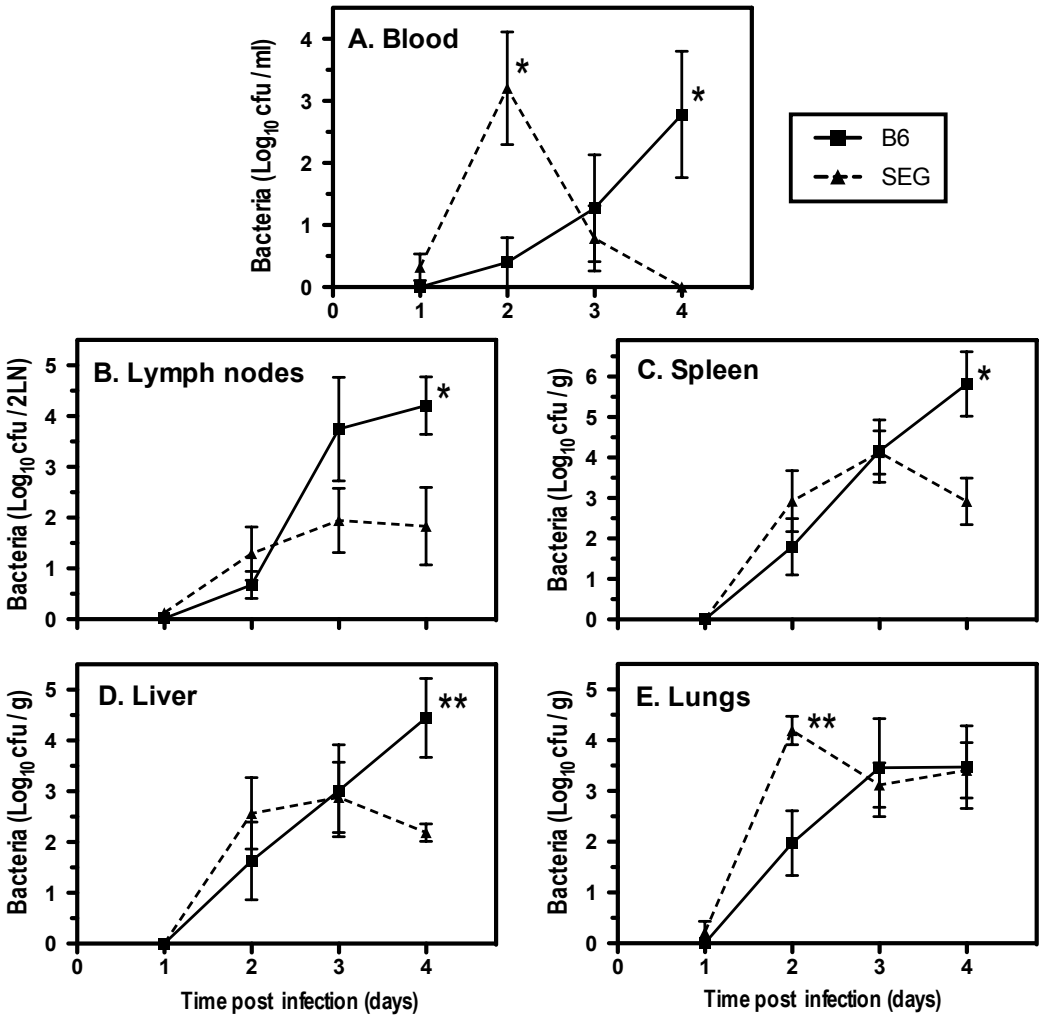


Figure 2

Click here to download Figure: C_Demeure_2011_Fig.2_JID2.pdf

Figure 2

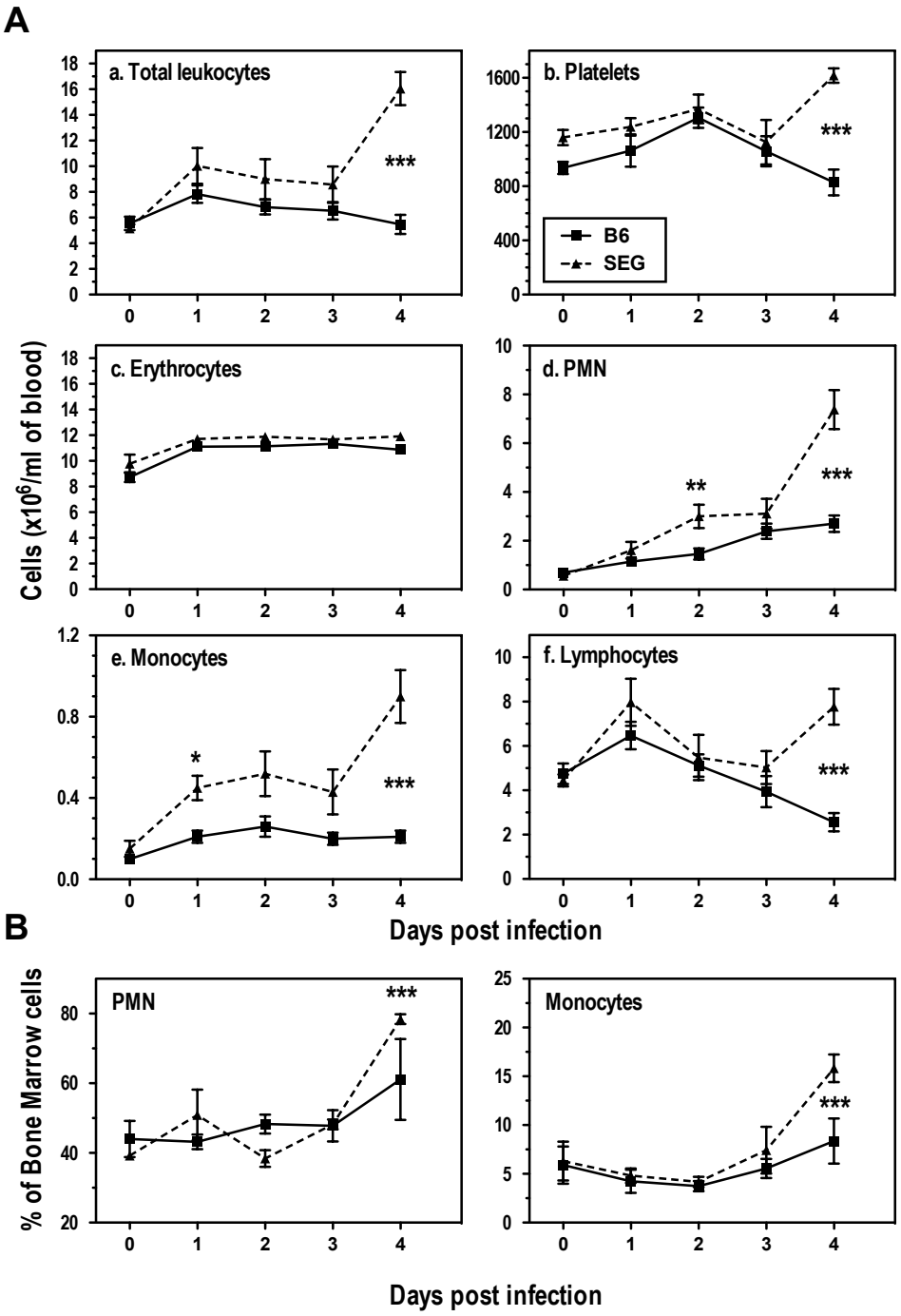


Figure 3

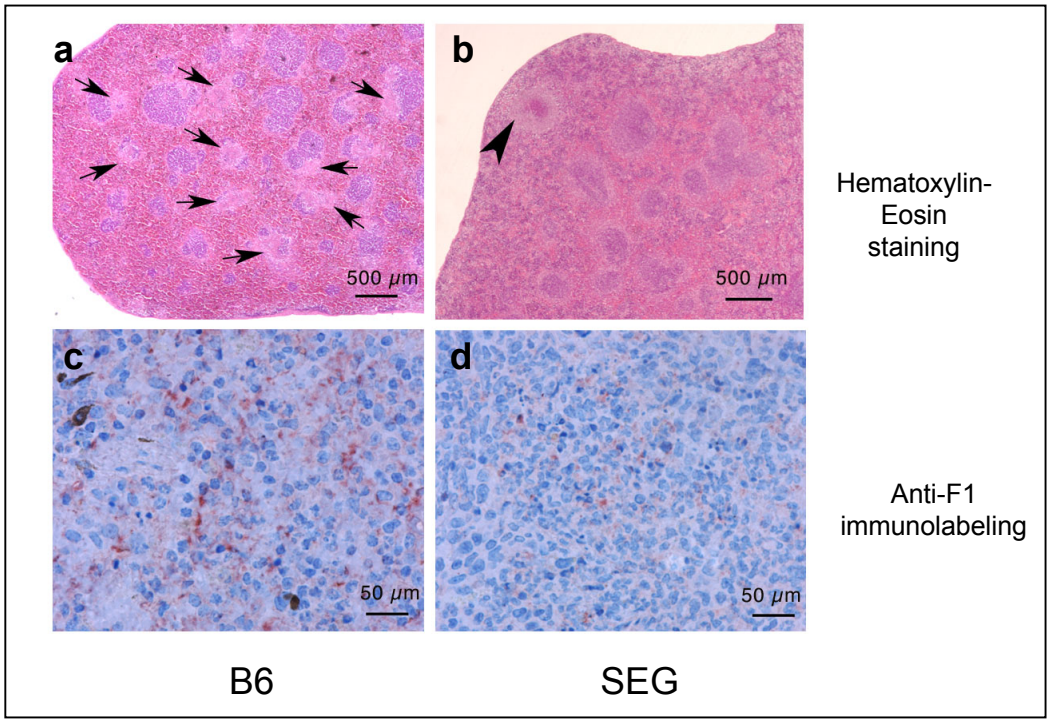
Click here to download Figure: C_Demeure_2011_Fig.3_JID2.pdf

Figure 3

A

	Day 1		Day 2		Day 3		Day 4	
	B6	SEG	B6	SEG	B6	SEG	B6	SEG
Mean score								
Hemorrages	0	0	0.6 (±0.1) *	0.2 (±0.1)	1.0 (±0.1) **	0.3 (±0.1)	1.0 (±0.2)	0.4 (±0.2)
PMN infiltrates	0.3 (±0.1)	0.3 (±0.1)	0.6 (±0.1)	0.5 (±0.1)	1.3 (±0.2) *	0.9 (±0.1)	1.9 (±0.5)	1.3 (±0.2)
Nb of mice affected/total								
Congestion	1/10	1/10	0/10	0/10	2/10	4/10	3/9	2/10
Necrosis	0/10	0/10	0/10	0/10	0/10	0/10	3/9	0/10
Micro abscesses	0/10	0/10	0/10	0/10	1/10	1/10	0/9	3/10

B



C

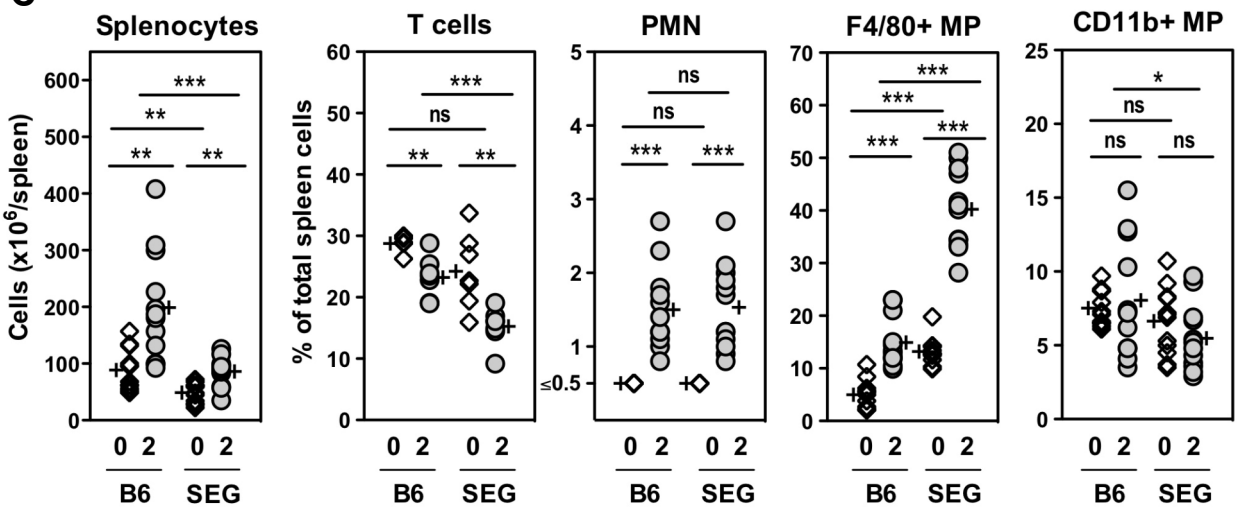


Figure 4

Click here to download Figure: C_Demeure_2011_Fig.4_JID2.pdf

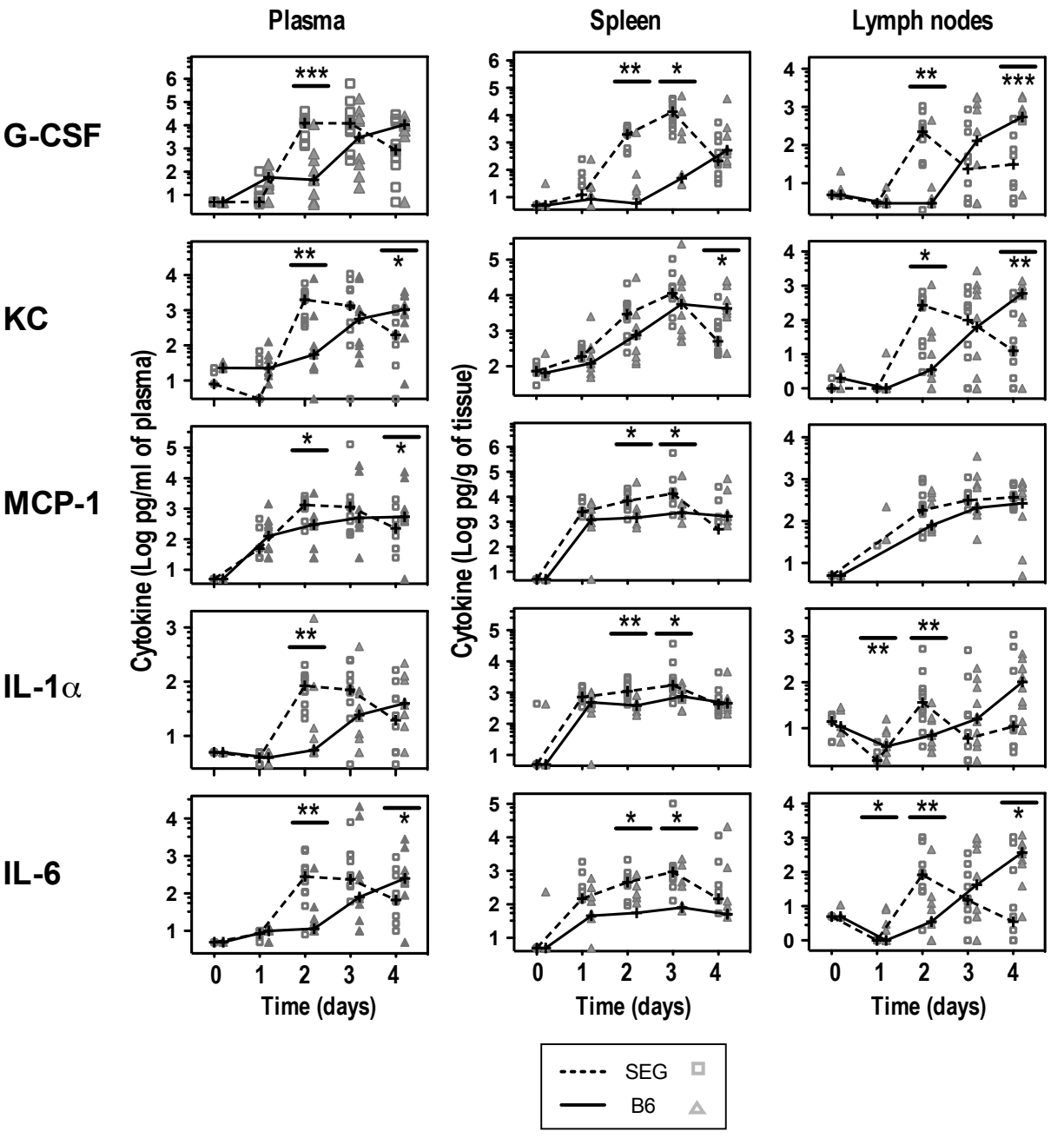
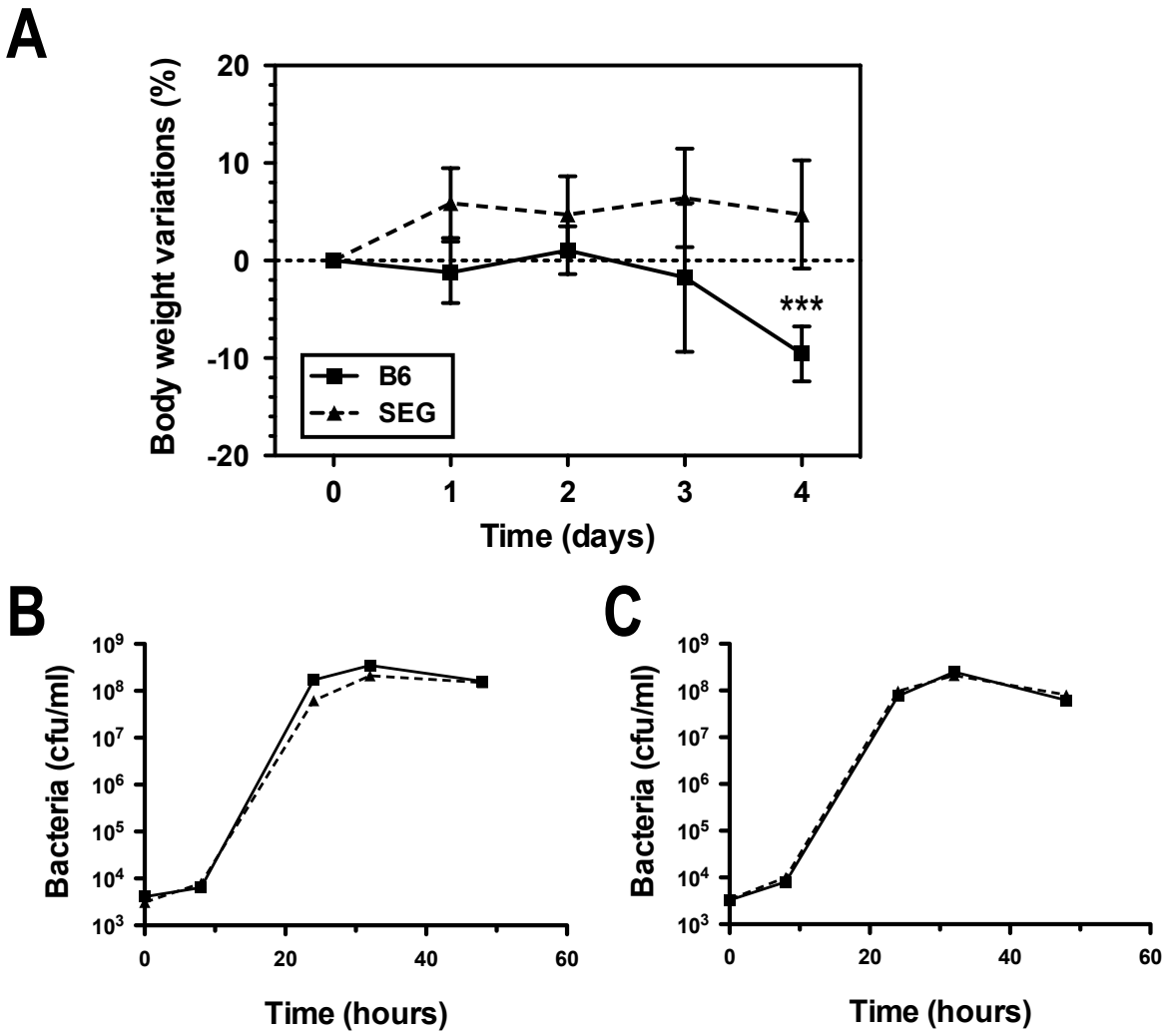
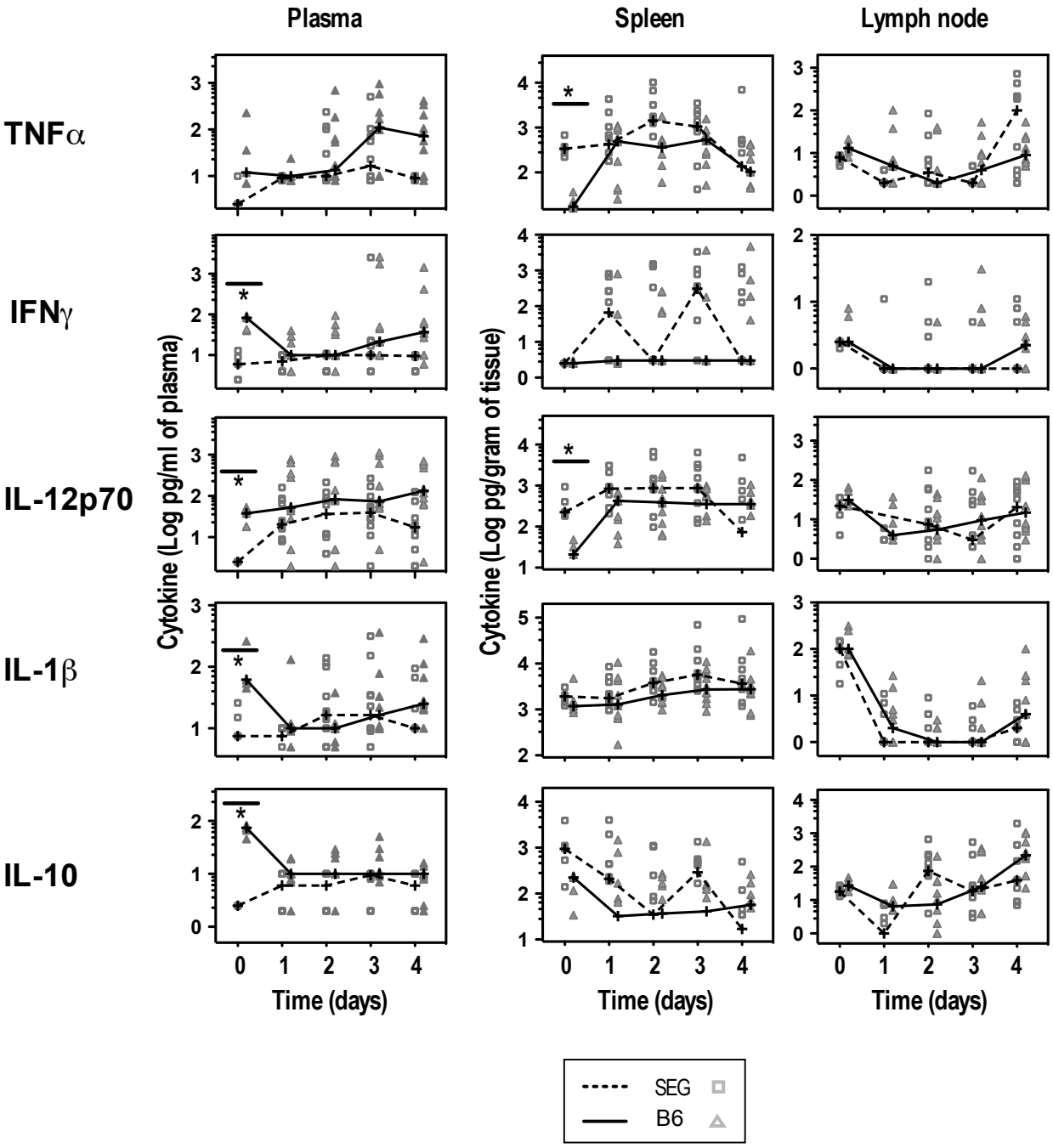


Figure S1
Click here to download Figure: C_Demeure_2011_Fig.S1_JID2.pdf



Supplementary figure S1: Comparison of B6 and SEG mice for body weight variations during infection and growth of *Y. pestis* in their serum
The weight of each animal was recorded daily after infection (A) and variation was calculated using the weight at day 0 as a reference. Shown are means ± sem of 9-10 mice per time point and per mouse strain. Stars indicate significant diffrences between the two mouse strains at a given time point determined using the Mann-Whitney-Wilcoxon rank sum test. ***: $p<0.001$. To determine the contribution of serum to the control of bacteremia by SEG mice, pools of undecomplemented sera collected from SEG or B6 mice prior to infection (B), or two days post infection (C) were inoculated with 10^3 cfu/ml of *Y. pestis* CO92 and incubated at 37°C. Serum aliquots were taken at different time points for bacterial count determination.

Figure S2
Click here to download Figure: C_Demeure_2011_Fig.S2_JID2.pdf



Supplementary Figure S2: Cytokine contents in the plasma, inguinal lymph nodes and spleen of B6 and SEG during the course of a *Y. pestis* infection.
Shown are the values for TNFα, IFNγ, IL-12p70, IL-1β, and IL-10 in 10 individual SEG (grey rectangles) or B6 (grey triangles, 9 animals for B6 on D4) mice from D0 to D4 pi, and the median curves (plain lines for B6, and dotted lines for SEG). The Wilcoxon statistical test was used to compare groups. *: $p \leq 0.05$. Stars above the comparison bar indicate values significantly superior in SEG, while stars below the comparison bar indicate values significantly superior in B6.